Benzochromenones from the Marine Crinoid *Comantheria rotula* Inhibit Hypoxia-Inducible Factor-1 (HIF-1) in Cell-Based Reporter Assays and Differentially Suppress the Growth of Certain Tumor Cell Lines

Jingqiu Dai, Yang Liu, Hong Jia, Yu-Dong Zhou,* and Dale G. Nagle*

Department of Pharmacognosy, Research Institute of Pharmaceutical Sciences, School of Pharmacy, University of Mississippi, University, Mississippi 38677-1848

Received May 11, 2007

Hypoxia-inducible factor-1 (HIF-1) is a transcription factor that promotes tumor cell adaptation and survival under hypoxic conditions. HIF-1 is currently recognized as an important molecular target for anticancer drug discovery. The National Cancer Institute open repository of marine invertebrates and algae lipid extracts was evaluated using a T47D breast tumor cell-based reporter assay for HIF-1 inhibitory activity. Bioassay-guided fractionation of an active extract from a crinoid *Comantheria rotula* yielded seven benzo[*g*]chromen-4-one and benzo[*h*]chromen-4-one pigments (**1**–**7**). The structures of the new benzo[*g*]chromenone dimer 9,9′-oxybis-neocomantherin (**1**) and another new natural pigment **5** were deduced from spectroscopic and spectrometric data. The crinoid pigments significantly inhibited both hypoxia-induced and iron chelator-induced HIF-1 luciferase reporter activity in breast and prostate tumor cells. However, inhibition of HIF-1 in the reporter assay did not translate into a significant decrease in the expression of the downstream HIF-1 target, secreted vascular endothelial growth factor (VEGF). Compound **1** was found to inhibit tumor cell growth in the NCI 60-cell line panel (GI_{50} values of 1.6–18.2 μM), and compound **6** produced a unique pattern of tumor cell growth suppression. Five cell lines from different organs were hypersensitive to **6** (GI_{50} values of 0.29–0.62 μM), and three others were moderately sensitive (GI_{50} values of 2.2–5.1 μM), while the GI_{50} values for most other cell lines ranged from 20 to 47 μM. Crinoid benzo[*g*]chromenones were also found to scavenge radicals in a modified DPPH assay.

In solid tumors, hypoxic regions emerge when rapid tumor growth tips the balance between oxygen supply and consumption, which results in reduced oxygen levels. Clinical studies revealed that the prevalence of tumor hypoxia is an indicator of advanced disease stage, treatment resistance, and poor prognosis.[1] Currently, there is no approved drug that selectively targets tumor hypoxia. First discovered as a hypoxia-induced protein that upregulates the expression of erythropoietin,[2] the transcription factor hypoxia-inducible factor-1 (HIF-1) has become an important molecular target for the discovery of drugs that target tumor hypoxia.[3] The availability and activity of the oxygen-regulated HIF-1α subunit plays a major regulatory role in the bioactivity of HIF-1, relative to that of the constitutively expressed subunit HIF-1β. Clinically, overexpression of the oxygen-regulated HIF-1α subunit is associated with advanced stage tumors and elevated metastasis.[4] In animal models, inhibiting HIF-1 through genetic or small molecule-based approaches suppresses tumor growth and improves the treatment outcome in adjunct therapy with either radiation or chemotherapeutic agents.[5–11] Because HIF-1 is not activated in well-oxygenated normal tissues, small molecule HIF-1 inhibitors have the potential to selectively target tumor cells while sparing normal cells. As a result of intensive research efforts to discover small molecule HIF-1 inhibitors, a number of chemically diverse small molecules that target various cellular pathways have been reported to inhibit HIF-1 function.[3,12,13] A large percentage of known small molecule HIF-1 inhibitors are either natural products or derived from natural products.

Our HIF-1 inhibitor discovery efforts have been focused on utilizing the biochemical diversity afforded by natural products, in combination with cell-based screening assays. The National Cancer Institute (NCI) open repository of marine invertebrates and algae lipid extracts was evaluated for HIF-1 inhibitory activity. The crude extract of a Papua New Guinea collection of the crinoid *Comantheria rotula* A. H. Clark (Comasteridae) inhibited hypoxia-induced HIF-1 activation (99% inhibition at 5 μg mL^{-1} in a T47D human breast tumor cell-based reporter assay). Bioassay-guided chromatographic separation of the *C. rotula* extract produced seven 4*H*-benzo[*g*]chromen-4-one and 4*H*-benzo[*h*]chromen-4-one pigments (**1**–**7**), which included five previously reported crinoid metabolites. The structures of two new crinoid pigments (**1** and **5**) were elucidated by analysis of spectroscopic and spectrometric data. Herein, we describe the isolation, structure elucidation, and biological characterization of these compounds.

Table 1. Compound **1** ^{13}C and ^{1}H NMR Data[a]

position	δ_C	δ_H
2/2′	168.3	
3/3′	112.6	6.13 s
4/4′	178.5	
5/5′	160.2	
6/6′	170.7	
7/7′	103.9	6.01 s
8/8′	178.2	
9/9′	134.4	
10/10′	116.5	7.95 s
11/11′	175.9	
12/12′	123.4	
13/13′	119.8	
14/14′	159.5	
15/15′	35.4	2.56 (t, 7.2)
16/16′	19.8	1.73 m
17/17′	13.4	1.03 (t, 7.2)
5/5′-OC$\underline{H}_3$	63.6	4.03 s
6/6′-OC$\underline{H}_3$	57.2	3.90 s

[a] $CDCl_3$; 100 MHz for ^{13}C; 400 MHz for ^{1}H.

Results and Discussion

The optically inactive compound **1** was obtained as a yellow powder with the molecular formula $C_{36}H_{34}O_{11}$, as deduced from analysis of high-resolution electrospray ionization mass spectrometry (HRESIMS) data. The ^{1}H nuclear magnetic resonance (NMR) spectrum (Table 1) exhibitedthe presence of three methyl group resonances at δ 1.03 ppm (t, J = 7.2 Hz), 3.90 ppm (s), 4.03 ppm (s), and three aromatic methine resonances. The ^{13}C NMR spectrum of **1** (Table 1) showed resonances for 18 carbons, and the ^{13}C DEPT spectrum indicated the presence of 3 methyl, 2 methylene, 3

* To whom correspondence should be addressed. Tel: (662) 915-7026. Fax: (662) 915-6975. E-mail: ydzhou@olemiss.edu (Y.-D.Z.). Tel: (662) 915-7026. Fax: (662) 915-6975. E-mail: dnagle@olemiss.edu (D.G.N.).

10.1021/np070224w CCC: $37.00
Published on Web 09/11/2007

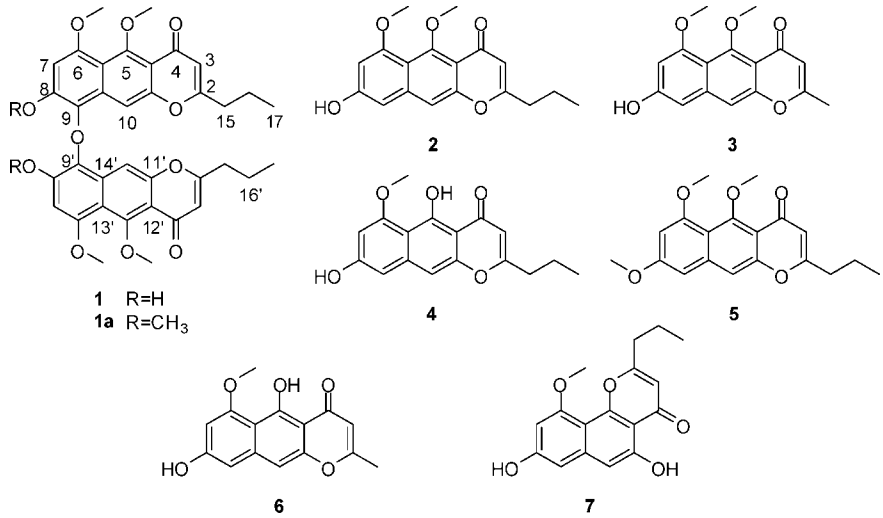

methine, and 10 quaternary carbon atoms. However, this was only half of the number of the carbon resonances expected from the molecular formula. This indicated that the structure was that of a symmetrically substituted dimer. The 2D NMR spectra [^{1}H–^{1}H correlation spectroscopy (COSY), ^{1}H–^{13}C heteronuclear multiple-quantum coherence (HMQC), and ^{1}H–^{13}C heteronuclear multiple-bond correlation (HMBC)] of **1** were strikingly similar to those of **2**, which was determined to be the known crinoid pigment neocomantherin (8-hydroxy-5,6-dimethoxy-2-propyl-4*H*-benzo[*g*]-chromen-4-one) by comparison with previously published ^{1}H and ^{13}C NMR data from the literature.[14] This suggested that **1** was a dimeric neocomantherin-like structure. The spectroscopic data from **1** were analyzed with respect to the location of the functional hydroxy and methoxy groups and the connectivity patterns of the two naphthalene systems. Analysis of the ^{1}H–^{13}C HMBC spectrum of **1** (Figure 1) revealed the presence of long-range ^{1}H–^{13}C couplings between the following: C-2 to H-3, H-15, and H-16; C-5 to C-5–OC$\underline{H}_3$; C-6 to H-7 and C-6–OC$\underline{H}_3$; C-8 to H-7; C-9 to H-7 and H-10; C-11 to H-10; C-12 to H-3 and H-10; and C-13 to H-7 and H-10. Methylation of the C-8 hydroxy group was easily performed by treatment of **1** with MeOH/H_2SO_4 to afford **1a**. The downfield change in the ^{1}H chemical shift observed for the H-7 resonance from δ 6.01 (**1**) to δ 6.16 (**1a**) was consistent with the proposed structure, in which the free hydroxy groups were located at C-8. Thus, the structure of **1** was deduced to be 9,9′-oxybis(8-hydroxy-5,6-dimethoxy-2-propyl-4*H*-benzo[*g*]chromen-4-one and assigned the trivial name 9,9′-oxybis-neocomantherin.

Compound **5** was obtained as a yellow powder with the molecular formula $C_{19}H_{20}O_5$, as deduced from analysis of the HRESIMS and ^{13}C NMR spectroscopic data. The ^{1}H NMR spectrum (Table 2) exhibited the presence of four methyl resonances, of which three were oxygen-substituted singlets (δ 3.91, 3.98, and 3.98) and one was a triplet (δ 1.04, t, J = 7.2 Hz). Four aromatic methine resonances were observed. The ^{13}C NMR spectrum of **5** (Table 2) contained resonances for 19 carbons, and the ^{13}C DEPT spectrum indicated the presence of four methyl, two methylene, four methine,

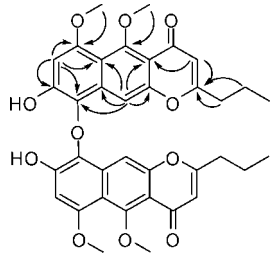

Figure 1. Selected HMBC (H → C) correlations of **1**.

Table 2. Compound **5** ^{13}C and ^{1}H NMR Data[a]

position	δ_C	δ_H
2	167.2	
3	109.8	6.01 s
4	178.2	
5	160.6	
6	159.5	
7	97.2	6.43 s
8	160.5	
9	98.8	6.62 s
10	108.4	7.37 s
11	154.7	
12	114.0	
13	114.4	
14	139.8	
15	35.4	2.53 (t, 7.2)
16	19.8	1.76 m
17	13.4	1.04 (t, 7.2)
5-OC$\underline{H}_3$	63.6	3.98 s
6-OC$\underline{H}_3$	57.2	3.91 s
8-OC$\underline{H}_3$	55.4	3.98 s

[a] $CDCl_3$; 100 MHz for ^{13}C; 400 MHz for ^{1}H.

and nine quaternary carbon atoms. The spectra of **5** were also similar to those of neocomantherin (**2**). The main differences in the NMR spectra of the two compounds were that the spectra of **5** contained ^{1}H and ^{13}C resonances (at δ 3.98 and 55.4 ppm, respectively) that were consistent with the presence of an additional C-8 methoxyl group substitution. This suggested that **5** was a new natural product 8-*O*-methylneocomantherin, which had been previously produced only through synthetic efforts.[15]

Three other previously reported benzo[*g*]chromenone-4-one crinoid pigments comantherin (**3**),[14] 5,8-dihydroxy-6-methoxy-2-propyl-4*H*-benzo[*g*]chromen-4-one (**4**),[16] and TMC-256A1 (**6**)[17] and the known benzo[*h*]chromenone-4-one pigment comaparvin (**7**)[16] were also isolated and identified by a comparison of their ^{1}H and ^{13}C NMR spectra with those reported in the literature.

The effects of **1**–**7** on HIF-1 activity were first examined in a cell-based reporter assay.[18] Compounds **1**–**7** significantly inhibited both hypoxia-induced and iron-chelator-induced HIF-1 activation (pHRE-TK-Luc) in T47D breast tumor cells (IC_{50} values of 1.7–7.3 μM for hypoxia-induced and 0.6–3.0 μM for 1,10-phenanthroline-induced HIF-1 activation; Table 3). Compounds **1**–**4** and **6** also inhibited hypoxia-induced HIF-1 activation (pHRE-TK-Luc) in PC-3 prostate tumor cells (IC_{50} values of 1.0–10.0 μM; Table 3). The IC_{50} values for **1**, **2**, **4**, and **6** to inhibit 1,10-phenanthroline-induced HIF-1 activation in PC-3 cells range from 0.8 to 3.9 μM (Table 3). Unlike any of the natural product-based HIF-1 inhibitors previously discovered through the use of this assay system,[18–22] compounds **1**–**6** show selectivity for iron chelator (1,10-phenan-

Table 3. IC_{50} Values (μM) of **1–7** on Luciferase Expression from the HIF-1-Regulated pHRE-TK-Luc and Control (pGL3-Control) Constructs

	T47D			PC-3		
	pHRE-TK-Luc		pGL3-control	pHRE-TK-Luc		pGL3-control
	1,10-phen	hypoxia	hypoxia	1,10-phen	hypoxia	hypoxia
1	0.8	7.3	7.5	3.9	10.0	>10.0
2	1.9	2.7	9.0	3.7	3.2	4.7
3	2.7	2.9	>10.0	>10.0	10.0	>10.0
4	0.6	1.7	7.0	0.8	1.0	2.8
5	2.0	3.9	>10.0	>10.0	>10.0	>10.0
6	0.9	3.4	>10.0	2.5	3.3	>10.0
7	3.0	3.0	>10.0	>10.0	>10.0	>10.0

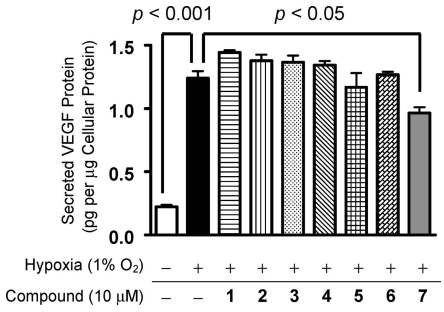

Figure 2. Effects of **1–7** on hypoxic induction of secreted VEGF protein(s) in T47D cells. Exponentially grown T47D cells were exposed to hypoxic conditions (1% O_2) in the presence of **1–7** (10 μM) for 16 h. Levels of secreted VEGF protein(s) in the conditioned media were determined by ELISA and normalized to cellular protein levels. Data shown are mean from one experiment performed in triplicate, and bars represent standard deviation. The *p* values were obtained using ANOVA analysis followed by Bonferroni's multiple comparison test (GraphPad Prism 4).

throline)-induced HIF-1 activation (mean IC_{50} of 1.7 μM; IC_{50} range of 0.6–3.0 μM) relative to hypoxia-induced HIF-1 activation (mean IC_{50} of 3.6 μM; IC_{50} range of 1.7–7.3 μM) in this cell-based reporter assay system.

Vascular endothelial growth factor (VEGF), a downstream gene that is regulated by HIF-1, is perhaps the most potent angiogenic factor known.[23] Avastin, a therapeutic antibody that inhibits VEGF, is the first Food and Drug Administration (FDA)-approved anti-angiogenic drug for the treatment of cancer. Because secreted VEGF protein(s) is the bioactive form and hypoxia is a major physiological stimuli for VEGF production, the effects of **1–7** (10 μM) on hypoxic induction of secreted VEGF protein(s) were examined in T47D cells (Figure 2). The benzo[*h*]chromenone-4-one pigment comaparvin (**7**) decreased the hypoxic induction of secreted VEGF protein(s) by 27% at the concentration of 10 μM. None of the compounds (**1–7**) inhibited the induction of secreted VEGF protein by 1,10-phenanthroline in T47D cells (data not shown). Because only **7** partially suppressed hypoxic induction of secreted VEGF proteins, compounds **1–6** were further evaluated for their specificity and the possibility that these compounds may be "nuisance compounds" that directly interfere with luciferase-based assay systems. As shown in Table 3, compounds **1**, **2**, and **4** inhibited luciferase expression from the control construct (pGL3-control). It is possible that structurally similar yellow pigments may interfere with various light-based high-throughput screening (HTS) methods but do not exhibit activity in other forms of bioassays. For example, yellow-colored phenolic compounds from a marine hydroid have recently been demonstrated to inhibit the antitumor molecular target indoleamine 2,3-dioxygenase (IDO) activity in a spectrophotometric-based *in vitro* HTS assay, but IDO inhibition could not be demonstrated with these compounds in a yeast cell-based method.[24] To determine if benzo[*g*]chromenone-4-one and benzo[*h*]chromenone-4-one pigments could directly inhibit the luciferase reaction or directly interfere with the spectrophotometric measurement of luciferase activity, a concentration–response curve was established for each of the compounds using a purified luciferase standard (**1–7**; Figure 3). Compound **1** was the most potent inhibitor of the luciferase standard (IC_{50} of 2.4 μM), followed by **2** and **4** that only inhibited by 48% at the highest concentration (30 μM). The IC_{50} of **1** to inhibit the luciferase standard is within the range of effective concentrations in the cell-based HIF-1 reporter assays (Table 3). However, because the conditioned media that contained dissolved **1** were removed prior to the luciferase assay in the cell-based system, interference with the luciferase reaction is unlikely to account for more than a small portion of the observed inhibition in the cell-based system. For the remaining compounds, weak inhibition of the luciferase standard (IC_{50} > 30 μM) does not seem potent enough to explain the inhibition observed in the cell-based system (Table 3). Further, crinoid pigments do not appear to inhibit cell-based luciferase HTS assays by acting as nonspecific transcription or translation inhibitors, because this would result in a suppression of secreted VEGF protein(s) production.

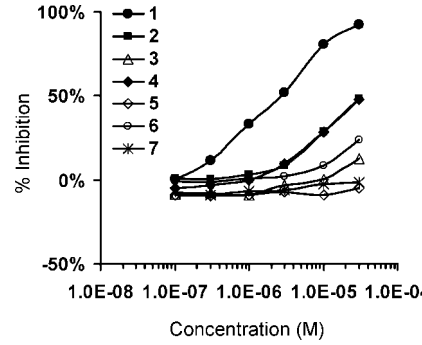

Figure 3. Effects of **1–7** on the activity of a luciferase standard. The activity of QuantiLum recombinant luciferase was measured in the presence and absence of compounds. Data were presented as a percentage inhibition of the solvent (DMSO) control. This experiment was performed in triplicate, and the standard deviation for each data point was less than 5% (not shown).

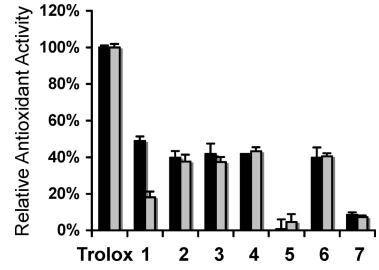

Figure 4. Radical scavenging activity of **1–7**. A modified 96-well plate-based DPPH assay was used to measure the radical scavenging activity. Data obtained from one experiment performed in triplicate were presented as relative antioxidant activity of the positive control Trolox, and the bars represent standard deviation. The black solid bars represent a compound/DPPH ratio of 1:1, and the gray solid bars represent a compound/DPPH ratio of 1:3.

Cellular oxygen sensing is commonly believed to be mediated by mitochondrial reactive oxygen species (ROS).[25,26] Therefore, certain radical scavengers may be able to inhibit HIF-1 signaling but otherwise exert very little effect on cells grown in culture. To test this hypothesis, compounds **1–7** were evaluated for their radical scavenging ability using a modified 1,1-diphenyl-2-picrylhydrazyl (DPPH) radical assay. The crinoid benzochromenones **1**−**4** and **6** were found to have about 40% of the DPPH radical scavenging capacity of the standard radical scavenger Trolox (Figure 4). Remarkably, compounds **1**−**4** and **6** were also the only crinoid

pigments that significantly inhibited HIF-1 activity in PC-3 prostate tumor cells (Table 3).

The effects of crinoid benzo[*g*]chromen-4-one pigments **1** and **3**–**6** on tumor cell proliferation and viability were examined in the NCI 60-cell line panel. Compound **1** inhibited tumor cell growth with a marginal level of selectivity (GI_{50} values of 1.6–18.2 μM; Supporting Information). Moreover, crinoid pigment **6** produced a unique pattern (0.54 Pearson correlation coefficient for the closest compound by COMPARE analysis) of tumor cell growth suppression. Five cell lines from different organs were hypersensitive to **6** (GI_{50} values of 0.295–0.62 μM), while the GI_{50} values for most other cell lines ranged from 20 to 47 μM (Supporting Information).

Because **1**–**6** inhibit HIF-1 reporter activity but do no decrease the production of the HIF-1 target-secreted VEGF protein(s), these pigments were not considered for further evaluation or development.

Experimental Section

General Experimental Procedures. The IR spectrum was obtained using an AATI Mattson genesis Series Fourier transform infrared spectroscopy (FTIR). The NMR spectra were recorded in $CDCl_3$ on a Bruker AMX-NMR spectrometer operating at 400 MHz for ^{1}H or 100 MHz for ^{13}C. The NMR spectra were recorded running gradients and using residual solvent peaks (δ 7.27 for ^{1}H) and (δ 77.0 for ^{13}C) as internal references. The HRESIMS spectra were measured using a Bruker Daltonic micro-time of flight (TOF) with electrospray ionization. Silica gel (200–400 mesh) was used for CC. Thin-layer chromatographies (TLCs) were run on Merck $Si_{60}F_{254}$ or $Si_{60}RP_{18}F_{254}$ plates and visualized under UV at 254 nm or by heating after spraying with a 1% anisaldehyde solution in acetic acid/H_2SO_4 (50:1).

Crinoid Material. The crinoid material was obtained from the NCI open repository program. *C. rotula* A. H. Clark (Comasteridae) samples were collected at 8 m depth on October 13, 1991 (collection C007979) from Papua New Guinea. The sample was collected by the Australian Institute of Marine Science and identified by Dr. R. Alistair Birtles (James Cook University, Townsville, Australia). It was frozen at −20 °C and ground in a meat grinder. A voucher specimen was placed on file with the Department of Invertebrate Zoology, National Museum of Natural History, Smithsonian Institution, Washington, D.C.

Extraction and Isolation. Ground *C. rotula* material was extracted with water. The residual sample was then lyophilized and extracted with CH_2Cl_2/MeOH (1:1); residual solvents were removed under vacuum; and the crude extract was stored at −20 °C in the NCI repository at the Frederick Cancer Research and Development Center (Frederick, Maryland). The crude extract of the marine crinoid (4 g) was separated into four fractions by Si gel CC (50 g), using a step gradient of hexanes in EtOAc (85:15, 50:50, and 0:100). Active fraction 4 [250 mg, which was originally eluted with hexanes/EtOAc (1:1)] was further separated by a second level of Si gel CC [hexanes/CH_2Cl_2/EtOAc (1:1:2)] to give **1** (10 mg, 0.25% yield), **2** (50 mg, 1.25% yield), and **3** (20 mg, 0.50% yield). Active fraction 3 [300 mg, which was originally eluted with EtOAc in hexanes (50:50)] was subjected to Si gel CC with EtOAc in hexanes (1:2) to give **4** (10 mg, 0.25% yield), **5** (20 mg, 0.50% yield), **6** (5.0 mg, 0.12% yield), **7** (30 mg, 0.75% yield), and an additional quantity of **2** (100 mg, 3.25% total yield).

9,9′-Oxybis-neocomantherin.

9,9′-Oxybis(8-hydroxy-5,6-dimethoxy-2-propyl-4*H*-benzo[*g*]chromen-4-one (1). Yellow powder. IR (KBr) υ_{max}: 3375, 1661, 1580 cm^{-1}. UV (CH_3OH) λ_{max} (log ε): 224 (4.42), 276 (4.61), 405 (3.81). ^{1}H and ^{13}C NMR data in Table 1. HRESIMS *m/z*: 665.1998 (M + Na^+) (calcd for $C_{36}H_{34}O_{11}$, 665.1997).

9,9′-Oxybis(5,6,8-trimethoxy-2-propyl-4*H*-benzo[*g*]chromen-4-one) (1a). Compound **1** (2 mg) was dissolved in MeOH (1 mL), and two drops of concentrated H_2SO_4 was added. The reaction mixture was stirred for 5 h at ambient temperature. The mixture was washed successively with diluted NaOH and water. The reaction product was purified by preparative TLC to give **1a** (1.5 mg). ^{1}H NMR ($CDCl_3$, 400 MHz) δ: 6.15 (s, H-3), 6.16 (s, H-7), 7.97 (s, H-10), 4.02 (s, 5-OC$\underline{H}_3$), 3.89 (s, 6-OC$\underline{H}_3$), 3.97 (s, 8-OC$\underline{H}_3$), 1.03 (t, J = 7.2 Hz, H-17), 1.76 (m, H-16), 2.57 (t, J = 7.2 Hz, H-15).

8-*O*-Methylneocomantherin.

5,6,8-Trimethoxy-2-propyl-4*H*-benzo[*g*]chromen-4-one (5). Yellow powder. IR (KBr) υ_{max}: 3370, 1660, 1475 cm^{-1}. UV (CH_3OH) λ_{max} (log ε): 253 (4.42), 276 (4.61), 405 (3.80). ^{1}H and ^{13}C NMR data in Table 2. HRESIMS *m/z*: 328.1380 (calcd for $C_{19}H_{20}O_5$, 328.1311).

Cell-Based Luciferase Assay. The T47D and PC-3 cells (ATCC) were maintained in DMEM/F12 media with glutamine (Mediatech) supplemented with 10% fetal calf serum [FCS, (v/v) Hyclone], 50 units mL^{-1} penicillin G sodium, and 50 μg mL^{-1} streptomycin (Biowhittaker) in a humidified environment under 5% CO_2/95% air at 37 °C. Transfection, compound treatment, exposure to hypoxic conditions, a hypoxia mimetic (10 μM 1,10-phenanthroline), and measurement of luciferase activity were performed as previously described.[18] The IC_{50} values were determined using GraphPad Prism 4 software from experiments performed in triplicate. Compounds were tested at half-log concentrations, and the standard deviation values for over 95% of the data points are less than 15%.

Enzyme-Linked Immunosorbent Assay (ELISA) for Secreted VEGF Protein(s). Plating of T47D cells, compound treatment, hypoxic exposure, and determination of secreted VEGF protein(s) level in the conditioned media were the same as those previously described.[18,19] The only modification is that the cells were lysed with 250 μL of M-PER mammalian protein extraction reagent (Pierce) after removal of the conditioned media, and protein concentrations in the cell lysates were determined using the Micro BCA protein assay kit (Pierce). The amount of secreted VEGF protein(s) was normalized to the amount of protein in the cellular lysates.

Luciferase Standard Assay. QuantiLum recombinat luciferase was purchased from Promega (E1701). The enzyme stock (14.4 mg mL^{-1}) was thawed on ice and diluted in assay buffer [1× passive lysis buffer (Promega) supplemented with BSA (1 mg mL^{-1})]. For luciferase activity determination, an equal volume of luciferase substrate (Promega, E1501) was added to a mixture of QuantiLum recombinat luciferase (46.8 μg mL^{-1}) and compound in the assay buffer. Light output was measured on a BioTek Synergy HT plate reader. The data were presented as a percentage inhibition of the solvent dimethylsulfoxide (DMSO)-treated control.

DPPH Radical Scavenger Assay. Compounds were prepared as stock solutions in DMSO (4 mM for **1**–**7** and 30 mM for Trolox) and diluted with isopropanol to achieve the final concentration. A mixture of compound and DPPH in isopropanol was added to 96-well plates in a volume of 200 μL/well, and light absorbance at 515 nm (OD_{515}) was measured on a BioTek Synergy HT plate reader. The following formula was used to calculate the radical scavenging activity: [1 − OD_{515}(compound)/OD_{515}(control)] × 100. The formula for relative radical scavenging activity was [activity(compound)/activity(Trolox)] × 100. Test compounds were evaluated at a final concentration of 10 μM and were examined using two different concentrations of DPPH (10 and 30 μM). Under experimental conditions, the solvent (DMSO) had no effect. Trolox and DPPH were purchased from Sigma.

Acknowledgment. The authors thank the Natural Products Branch Repository Program at the NCI for providing marine extracts from the NCI open repository used in these studies, D. J. Newman and E. C. Brown (NCI, Frederick, MD) for assistance with sample logistics and collection information, J. A. Beutler (NCI, Frederick, MD) for COMPARE analysis, T. Smillie (University of Mississippi) for coordinating sample acquisition from the NCI, D. K. Jones and J. A. Fishback (University of Mississippi) for initial screening samples in the HIF-1 assay, and S. L. McKnight (UT Southwestern Medical Center at Dallas) for providing the pTK-HRE3-luc construct. This work was supported by the NIH-NCI CA 98787 (to D.G.N. and Y.-D.Z.), the Department of Defense (DOD)-Prostate Cancer Research Program PC040931 (to D.G.N.), and NOAA NURP/NIUST NA16RU1496. This investigation was conducted in a facility constructed with support from Research Facilities Improvement Grant C06 RR-14503-01 from the National Institutes of Health (NIH). The U.S. Army Medical Research Acquisition Activity, 820 Chandler Street, Fort Detrick, MD 21702-5014 is the awarding and administering acquisition office for the DOD support. The content herein reported does not necessarily reflect the position or the policy of the Government, and no official endorsement should be inferred.

Supporting Information Available: NCI/DTP 60-cell line GI_{50}, TGI, and LC_{50} mean bar graphs for **1** and **3**–**6**. The material is available free of charge via the Internet at http://pubs.acs.org.

References and Notes

(1) Tatum, J. L.; Kelloff, G. J.; Gillies, R. J.; Arbeit, J. M.; Brown, J. M.; Chao, K. S.; Chapman, J. D.; Eckelman, W. C.; Fyles, A. W.; Giaccia, A. J.; Hill, R. P.; Koch, C. J.; Krishna, M. C.; Krohn, K. A.; Lewis, J. S.; Mason, R. P.; Melillo, G.; Padhani, A. R.; Powis, G.; Rajendran, J. G.; Reba, R.; Robinson, S. P.; Semenza, G. L.; Swartz, H. M.; Vaupel, P.; Yang, D.; Croft, B.; Hoffman, J.; Liu, G.; Stone, H.; Sullivan, D. *Int. J. Radiat. Biol.* **2006**, *82*, 699–757.
(2) Semenza, G. L.; Wang, G. L. *Mol. Cell. Biol.* **1992**, *12*, 5447–5454.
(3) Semenza, G. L. *Expert Opin. Ther. Targets* **2006**, *10*, 267–280.
(4) Zhong, H.; De Marzo, A. M.; Laughner, E.; Lim, M.; Hilton, D. A.; Zagzag, D.; Buechler, P.; Isaacs, W. B.; Semenza, G. L.; Simons, J. W. *Cancer Res.* **1999**, *59*, 5830–5835.
(5) Maxwell, P. H.; Dachs, G. U.; Gleadle, J. M.; Nicholls, L. G.; Harris, A. L.; Stratford, I. J.; Hankinson, O.; Pugh, C. W.; Ratcliffe, P. J. *Proc. Natl. Acad. Sci. U.S.A.* **1997**, *94*, 8104–8109.
(6) Ryan, H. E.; Lo, J.; Johnson, R. S. *EMBO J.* **1998**, *17*, 3005–3015.
(7) Ryan, H. E.; Poloni, M.; McNulty, W.; Elson, D.; Gassmann, M.; Arbeit, J. M.; Johnson, R. S. *Cancer Res.* **2000**, *60*, 4010–4015.
(8) Kung, A. L.; Wang, S; Klco, J. M.; Kaelin, W. G.; Livingston, D. M. *Nat. Med.* **2000**, *6*, 1335–1340.
(9) Kung, A. L.; Zabludoff, S. D.; France, D. S.; Freedman, S. J.; Tanner, E. A.; Vieira, A.; Cornell-Kennon, S.; Lee, J.; Wang, B.; Wang, J.; Memmert, K.; Naegeli, H. U.; Petersen, F.; Eck, M. J.; Bair, K. W.; Wood, A. W.; Livingston, D. M. *Cancer Cell* **2004**, *6*, 33–43.
(10) Unruh, A.; Ressel, A.; Mohamed, H. G.; Johnson, R. S.; Nadrowitz, R.; Richter, E.; Katschinski, D. M.; Wenger, R. H. *Oncogene* **2003**, *22*, 3213–3220.
(11) Moeller, B. J.; Dreher, M. R.; Rabbani, Z. N.; Schroeder, T.; Cao, Y.; Li, C. Y.; Dewhirst, M. W. *Cancer Cell* **2005**, *8*, 99–110.
(12) Nagle, D. G.; Zhou, Y.-D. *Curr. Drug Target* **2006**, *7*, 355–369.
(13) Melillo, G. *Cancer Metastasis Rev.* 2007, *26*, 341–352.
(14) Kent, R. A.; Smith, I. R.; Sutherland, M. D. *Aust. J. Chem.* **1970**, *23*, 2325–2335.
(15) Rideout, J. A.; Smith, I. R.; Sutherland, M. D. *Aust. J. Chem.* **1976**, *29*, 1087–1098.
(16) Francesconi, K. A. *Aust. J. Chem.* **1980**, *33*, 2781–2784.
(17) Sakurai, M.; Kohno, J.; Yamamoto, K.; Okuda, T.; Nishio, M.; Kawano, K.; Ohnuki, T. *J. Antibiot.* **2002**, *55*, 685–692.
(18) Hodges, T. W.; Hossain, C. F.; Kim, Y.-P.; Zhou, Y.-D.; Nagle, D. G. *J. Nat. Prod.* **2004**, *67*, 767–771.
(19) Mohammed, K. A.; Hossain, C. F.; Zhang, L.; Bruick, R. K.; Zhou, Y.-D.; Nagle, D. G. *J. Nat. Prod.* **2004**, *67*, 2002–2007.
(20) Zhou, Y.-D.; Kim, Y.-P.; Mohammed, K. A.; Jones, D. K.; Muhammad, I.; Dunbar, D. C.; Nagle, D. G. *J. Nat. Prod.* **2005**, *68*, 947–950.
(21) Hossain, C. F.; Kim, Y.-P.; Baerson, S. R.; Zhang, L.; Bruick, R. K.; Mohammed, K. A.; Agarwal, A. K.; Nagle, D. G.; Zhou, Y.-D. *Biochem. Biophys. Res. Commun.* **2005**, *333*, 1026–1033.
(22) Dai, J.; Fishback, J. A.; Zhou, Y.-D.; Nagle, D. G. *J. Nat. Prod.* **2006**, *69*, 1715–1720.
(23) Ferrara, N.; Gerber, H. P.; LeCouter, J. *Nat. Med.* **2003**, *9*, 669–676.
(24) Pereira, A.; Vottero, E.; Roberge, M.; Mauk, A. G.; Andersen, R. J. *J. Am. Chem. Soc.* **2006**, *128*, 16046–16047.
(25) Simon, M. C. *Adv. Exp. Med. Biol.* **2006**, *588*, 165–170.
(26) Guzy, R. D.; Schumacker, P. T. *Exp. Physiol.* **2006**, *91*, 807–819.

NP070224W